Available online at www.sciencedirect.com
SCIENCE DIRECT®
PERGAMON
Materials Science in Semiconductor Processing 6 (2003) 205–208
MATERIALS SCIENCE IN SEMICONDUCTOR PROCESSING

{3 1 1} Defect evolution in Si-implanted $Si_{1-x}Ge_x$ alloys

Robert T. Crosby[a,*], Kevin S. Jones[a], Mark E. Law[a], A. Nylandsted Larsen[b], J. Lundsgaard Hansen[b]

[a] University of Florida, SWAMP Group Gainesville, FL 32611,Gainesville, FL, USA
[b] Institute of Physics and Astronomy, University of Aarhus, DK-8000, Aarhus, Denmark

Abstract

Molecular beam epitaxial (MBE), unstrained $Si_{1-x}Ge_x$ layers of various Ge concentrations, ranging from 0% to 50%, were grown on top of a $\langle 1\,0\,0 \rangle$ Si substrate. The wafers were subjected to a 10 keV, $1 \times 10^{14}\,cm^{-2}\,Si^+$ non-amorphizing implant. To study the defect morphology, the samples were annealed at 750°C for a total of 180 min. Plan-view transmission electron microscopy (PTEM) was utilized to observe and quantify the formation and dissolution of the defects. The $Si_{1-x}Ge_x$ samples with $\leqslant 5\%$ Ge exhibited {3 1 1} defect formation and dissolution; however, samples with Ge fractions $\geqslant 25\%$ showed only dislocation loop formation likely caused by a decrease in bond strength with increasing Ge content.

Keywords: $Si_{1-x}Ge_x$ alloys; {3 1 1} defect; Plan-view transmission electron microscopy (PTEM)

1. Introduction

Many novel electronic and optical device applications can be achieved through the extensive use of $Si_{1-x}Ge_x$ alloys [1–3] for two major reasons. First, adjustments in the composition of the alloy enable the band structure and mobility to be easily modified [4]. Second, since Si and Ge are isovalent materials with lattice constants differing by ~4%, a miscible alloy of the Si and Ge can be crystallized into a diamond lattice structure.

Defect studies of relaxed $Si_{1-x}Ge_x$ alloys are crucial to the semiconductor industry's understanding of the interaction of the various material components, i.e. Si, Ge, dopants, impurities, etc. Ion implantation and subsequent annealing are the key processing steps in the doping of semiconductor devices. It is well known that upon annealing implant damage in Si, the displaced ions can experience transient enhanced diffusion (TED) [5] resulting from the migration of remaining Si interstitials injected into the damaged region [6]. Under conventional annealing and non-amorphizing implantation practices, excess interstitials will form type I defects, i.e. {3 1 1} defects and dislocations loops around the projected range of the implant where the interstitial supersaturation is the highest [7,8]. {3 1 1} defects can be described as a monolayer of hexagonal Si serving as a reservoir for self-interstitials [9] that acts to minimize the number of dangling bonds [6]. TED in Si under the amorphization threshold is governed by the evolution of {3 1 1} defects [6,10]. Of late, the diffusion and activation of implanted semiconductors in relaxed $Si_{1-x}Ge_x$ has been intensely characterized [11–14], but very few have attempted to investigate the resulting defect morphology. It is imperative that the extended defects in these alloys be examined from a physical viewpoint. This paper will address the resulting defect evolution of injected and subsequently annealed interstitials in unstrained $Si_{1-x}Ge_x$ alloys.

2. Experiment

Relaxed $Si_{1-x}Ge_x$ wafers were grown by molecular beam epitaxy. The investigated Ge contents were: 0%, 2%, 5%, 25%, 35%, and 50%. Samples were grown by a "bottleneck" method to getter contaminants in the

*Corresponding author. Department of Materials Science & Engineering, Room 525 New Engineering Building PO Box 116130, Gainesville, FL 32601, USA. Tel.: +352-392-1019, fax: +352-392-8381.
E-mail address: rcros@mse.ufl.edu (R.T. Crosby).

1369-8001/03/$ - see front matter
doi:10.1016/S1369-8001(03)00087-8

epitaxially grown top Si layer, whereby a compositionally graded buffer layer incorporates Ge into the sample at an increasing rate of 10% Ge per micron at high growth temperatures around 750–800°C [15]. Alloyed layers of constant composition were lightly doped ($5 \times 10^{15}\,cm^{-3}$) with Sb and were approximately 1 μm in thickness. With the alloyed wafers, the Si cap was etched away, and the exposed $Si_{1-x}Ge_x$ layer was slightly lapped to smooth the surface. All samples were subjected to a 40 keV, $1 \times 10^{14}\,cm^{-2}$ non-amorphizing Si implant and thinned to attain plan-view transmission electron microscopy (PTEM) samples. Following PTEM preparation, these samples were annealed in a tube furnace under a N_2 ambient for 3 h at 750°C in discrete time intervals. Analysis was conducted via PTEM using a JEOL 200CX microscope with the defects imaged under weak beam, dark-field conditions at g_{220}, for defects are visible when $\boldsymbol{g} \cdot \boldsymbol{b} \times \boldsymbol{u} \neq \boldsymbol{0}$, where $\boldsymbol{g}$ is the reciprocal lattice vector corresponding to the diffraction plane, $\boldsymbol{b}$ is the Burger's vector of the dislocation, and $\boldsymbol{u}$ is the line direction of the dislocation. Loop density, {3 1 1} defect density, and the total trapped interstitial concentration were quantified to attain a correlation between defect growth and Ge content.

3. Results

To emphasize the difference in the ensuing defect structure from the various Ge concentrations, the work has been divided into two regimes: the low Ge concentration samples (0%, 2%, and 5%) and the high Ge concentration samples (25%, 35%, and 50%). Within 20–30 min of annealing, distinct {3 1 1} defects begin to form in the samples with low Ge concentrations. Representing PTEM images of the defect morphology resulting from a 750°C anneal of Si-implanted Si, Fig. 1(a–c) illustrates this trend. At 30 min, {3 1 1} defects are evident. Fifteen minutes later, the {3 1 1} defects have decreased in number, and a few, small dislocation loops become visible. At even longer times, the number of {3 1 1} defects continues to decrease leaving behind dislocation loops.

Fig. 1(d-f) displays the defect evolution of the $Si_{0.75}Ge_{0.25}$ alloy. At 30 min, dislocation loops are observed. At 45 min, it becomes apparent that the size of dislocation loops has increased. After 2 h of annealing, the density of dislocation loops appears to remain almost constant throughout the duration of the anneal. Only the size of the dislocation loops change slightly over time. No {3 1 1} defects are observed at higher Ge concentrations indicating that dislocation loop formation is highly preferential in the high Ge content regime.

Fig. 2a and b are a clear illustration that increasing the Ge concentration decreases the possibility of {3 1 1} defect formation. Fig. 2a shows the {3 1 1} defect density for the low Ge content regime, and Fig. 2b plots the ratio of {3 1 1} defects to dislocation loops formed for these samples, where $D_{\{3\,1\,1\}}$ denotes the defect density of {3 1 1} defects and D_{loop} represents the defect density

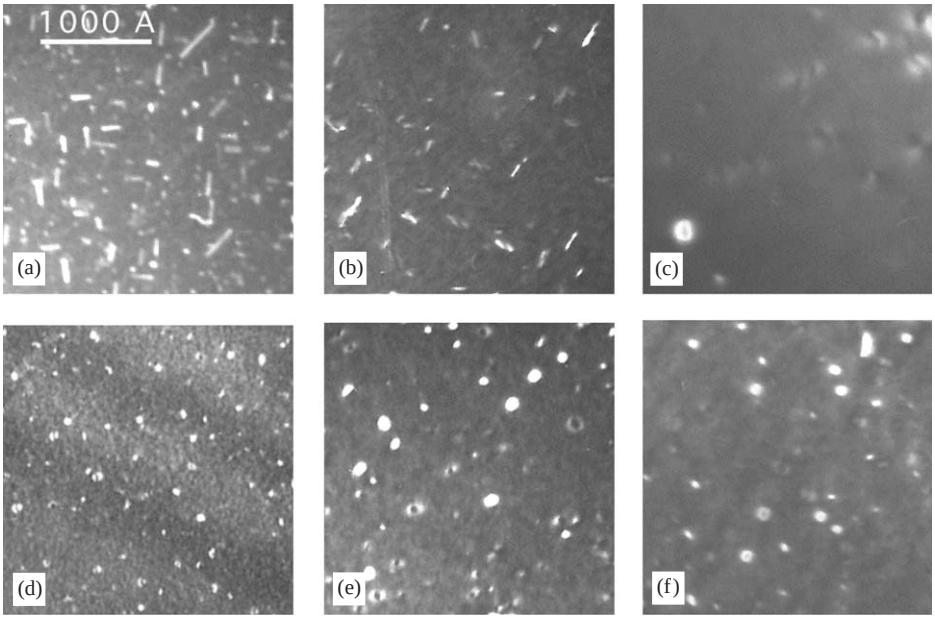

Fig. 1. PTEM images of 40 keV, $1 \times 10^{14}\,cm^{-2}$ Si implanted into pure Si annealed at 750°C for (a) 30 min, (b) 45 min, and (c) 120 min. PTEM images of 40 keV, $1 \times 10^{14}\,cm^{-2}$ Si implanted into relaxed $Si_{0.75}Ge_{0.25}$ annealed at 750°C for (d) 30 min, (e) 45 min, and (f) 120 min.

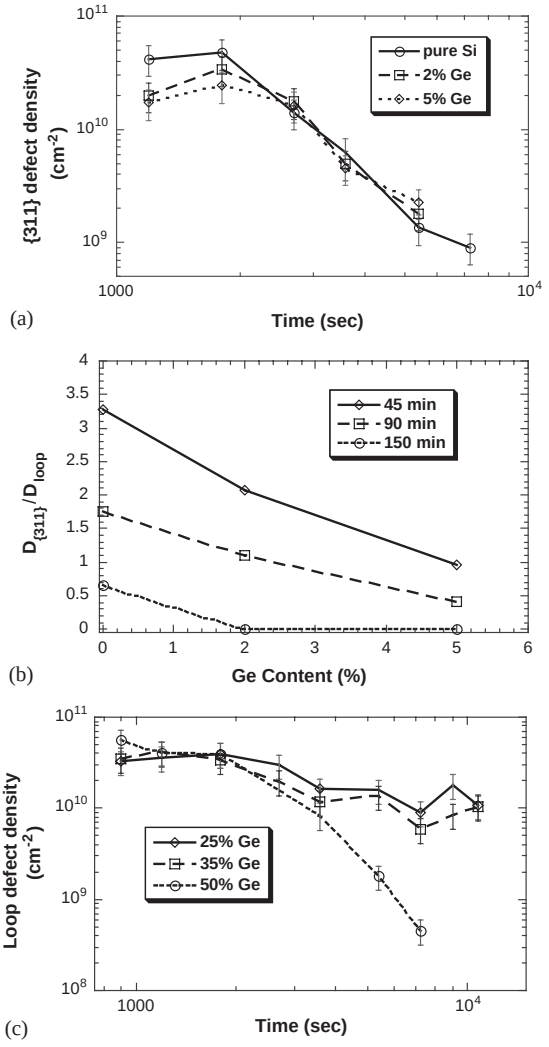

Fig. 2. (a) {3 1 1} defect density as a function of anneal time, (b) ratio of {3 1 1} defect density to dislocation loop defect density as a function of Ge content for the low Ge content regime, and (c) dislocation loop defect density as a function of anneal time.

of dislocation loops. It appears that dislocation loop formation is favored by adding Ge to the alloy. Dislocation loops stabilize earlier in the alloys than in pure Si. Discrete dislocation loops are not observed in Si at these implant and annealing conditions until around 45 and 60 min, whereas $Si_{0.95}Ge_{0.05}$ and $Si_{0.98}Ge_{0.02}$ show stable loop formation around 30 min. Exemplified by Fig. 2c, dislocation loops stabilize over longer periods of time for the $Si_{0.75}Ge_{0.25}$ and $Si_{0.65}Ge_{0.35}$ alloys. Above 35%, the dislocation loops are significantly less stable.

The total trapped interstitial concentration displayed in Fig. 3 follows an exponential decay and represents the sum of the trapped interstitials found in {3 1 1} defects and dislocation loops. Fig. 3 shows that the higher the

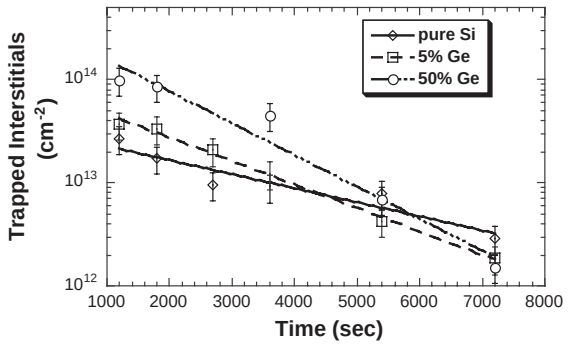

Fig. 3. Total trapped interstitial concentration as a function of anneal time for the pure Si, $Si_{0.95}Ge_{0.05}$, and $Si_{0.50}Ge_{0.50}$ with a 40 keV, $1 \times 10^{14}\,cm^{-2}$ Si implant annealed at 750°C.

Ge content the shorter the time constant for interstitial release. The concentration of trapped interstitials in extended defects can be described as: $C_i = C_0 \exp[-kt]$, where C_0 is the initial trapped interstitial concentration, t is the time of decay, and k is a decay constant [6]. The decay time constants of the pure Si, $Si_{0.95}Ge_{0.05}$, and $Si_{0.50}Ge_{0.50}$ alloys are 53, 32, and 23 min, respectively.

Early experiments predicted that dislocation loops are the result of unfaulting of {3 1 1} defects [16,17]. These experiments show that increasing the Ge concentration favors the formation of dislocation loops over {3 1 1} defects. This implies that with increasing Ge concentration either the unfaulting reaction of {3 1 1} defects is accelerated, or {3 1 1} defect formation is circumvented and the excess interstitials precipitate directly into dislocation loops. Since dislocation loops are observed at the shortest times for the higher Ge contents, it was impossible to determine which of these reactions dominated.

The observed effects of Ge on the microstructure may be the result of a change in the average bond strength of the alloy. It is known that increasing the Ge content reduces the melting point [18] and bond strength of the alloy [19]. The high energy associated with Si bonding is responsible for the stabilization of {3 1 1} defect formation [9]. It is reasonable to speculate that adding Ge to the alloy creates an increasingly unstable environment for {3 1 1} defect formation.

4. Conclusions

In summary, the defect morphology of the two separate regimes (i.e. $Si_{1-x}Ge_x$ samples with $\leqslant 5\%$ Ge and samples with Ge contents $\geqslant 25\%$) differs greatly. With the $Si_{0.98}Ge_{0.02}$ and $Si_{0.95}Ge_{0.05}$ alloys, {3 1 1} defects are observed, and the dissolution rates are comparable to that of pure Si. However, dislocation loop formation increases with Ge concentration. For the

intermediate Ge concentrated alloys, namely $Si_{0.75}Ge_{0.25}$ and $Si_{0.65}Ge_{0.35}$, dislocation loops appear relatively stable. When the Ge content is increased to 50%, the dislocation loops become unstable.

Acknowledgements

The authors would like to thank the SWAMP Group, J. Frazer for preparing the TEM samples, Varian Semiconductors for ion implantation, and the NSF and SRC for their support.

References

[1] Tatsumi T, Hirayama H, Aizaki N. Si/ $Ge_{.30}Si_{.70}$ heterojunction bipolar transistors made with Si molecular beam epitaxy. Appl Phys Lett 1988;52:895.

[2] Temkin H, Antreasyan A, Olsson NA, Pearsall TP, Bean JC. $Ge_{.60}Si_{.40}$ rib waveguide avalanche photodetectors for 1.3 μm operation. Appl Phys Lett 1986;49:809.

[3] MacWilliams KP, Plummer JD. Device physics and technology of complementary Si MESFET for VLSI applications. IEEE Trans Devices 1991;38:2619.

[4] Patton GL, Comfort JH, Meyerson BS, Crabbe EF, Scilla GJ, De Fresart E, Stork JC, Sun JYC, Harme DL, Burghartz JN. 75-GHz f_T SiGe-base heterojunction bipolar transistor. IEEE ED Lett 1990;11:171.

[5] Cowern NEB, Jannsen KTF, Jos HFF. Transient diffuison of Ion-implanted B in Si: dose, time, and matrix dependence of atomic and electrical profiles. J Appl Phys 1990;68:6191.

[6] Eagelsham DJ, Stolk PA, Gossmann H-J, Poate JM. Implantation and transient B diffusion in Si: the source of interstitials. Appl Phys Lett 1994;65:2305.

[7] Vandervorst W, Houghton DC, Shepherd FR, Swanson ML, Plattner HH, Carpenter GJC. Residual damage in B^+ and BF^{2+} implanted Si. Can J Phys 1985;63:863.

[8] Jones KS, Prussin S, Weber ER. A systematic Analysis of defects using ion-implanted Si. Appl Phys A 1988;45:1.

[9] Tan TY. Atomic modeling of homogenous nucleation of dislocation loops from condensation of point defects. Philos Mag A 1981;44:101.

[10] Rafferty CS, Gilmer GH, Jaraiz M, Eaglesham D, Gossmann H-J. , Simulation of cluster evaporation and transient enhanced diffusion in Si. Appl Phys Lett 1996;68:2395.

[11] Laitinen P, Strohm A, Huikari J, Voss T, Grodon C, Riihimäki I, Krummer M, Åystö J, Dendooven P, Räisänen J, Frank W. The ISOLDE collaboration self-diffusion of ^{31}Si and ^{71}Ge in relaxed $Si_{0.20}$ $Ge_{0.80}$ layers. Phys Rev Lett 2002;89:085902.

[12] Zangenberg NR, Lundsgaard Hansen J, Fage-Pedersen J, Nylandsted Larsen A. Ge self-diffusion in epitaxial $Si_{1-x}Ge_x$ layers. Phys Rev Lett 2001;87:125901.

[13] S Eguchi, CW Leitz, EA Fiztergerald, JL Hoyt. Diffusion behavior of ion-implanted n-type dopants in silicon germanium, Mater Res Soc Symp Proc 2002;686:A1.7.1.

[14] Thompson PE, Bennett J. Formation and thermal stability of ultra-shallow p^+ junctions in S_i and $Si_{1-x}Ge_x$ formed by molecular beam epitaxy. J Appl Phys 2002;92:6845.

[15] Nylandsted Larsen A, Kringhøj P, Lundsgaard Hansen J, Yu Shiryaev S. Impurity gettering in MBE grown silicon. Mater Res Soc Symp Proc 1995;378:285.

[16] Salisbury IG, Loretto MH. Loops in electron-irradiated Si. Philos Mag A 1979;39:317.

[17] Li J, Jones KS. {3 1 1} defects in Si: the source of loops. Appl Phys Lett 1998;73:3748.

[18] Olesinski RW, Abbaschian GJ. The Ge–Si system. Bull Alloy Phase Diag 1984;5:180.

[19] Tersoff J. Modeling solid state chemistry: interatomic potentials for multicomponent systems. Phys Rev B 1989;39:5566.